Chapter 6

Flexible Low-Voltage Carbon Nanotube Heaters and their Applications

Seyram Gbordzoe, Rachit Malik, Noe Alvarez,
Robert Wolf and Vesselin Shanov

Additional information is available at the end of the chapter

http://dx.doi.org/10.5772/64054

Abstract

Carbon nanotube heaters recently gained more attention due to their efficiency and relative ease of fabrication. In this chapter, we report on the design and fabrication of low-voltage carbon nanotube (CNT) heaters and their potential applications. CNT sheets drawn from CNT arrays have been used to make the heaters. The sheet resistance of the CNT sheet is dependent on the number of layers accumulated during their formation, and it ranges from 3.57 kΩ/sq. for a 1-layer sheet to 6.03 Ω/sq. for a 300-layer sheet. The fabricated and studied CNT heaters revealed fast heating and cooling rate. Potential applications of these heating devices have been illustrated by manufacturing and testing heatable gloves and via deicing experiments using low-voltage CNT heaters.

Keywords: CNT sheet, CNT heater, heated gloves

1. Introduction

Lightweight and low-power-consuming heaters that can be easily integrated in different materials and devices are needed for many industries including aerospace and medicine. The cold seasons usually bring the risk for several health problems, such as hypothermia, frostbite, flu, and even heart attacks. These adverse conditions make it difficult for people to conduct their daily routines effectively and safely during cold weather, due to the lack of proper gear to protect them. Some of the main attributes of a heating material, which can be safely incorporated into apparel, are lightweight, flexibility, fast heating rate, and energy efficiency. CNT sheets meet most of these qualities and thus are potential candidates as heating materials.

Carbon nanotubes have been the subject of immense interest since their official discovery in 1991 [1]. They attracted much attention due to their unique electrical, structural, mechanical and thermal conductivities, and their multiple potential applications [2–5]. It has been shown that CNT arrays can be processed into yarns and sheets, which have excellent properties [6–11]. One of the newer applications of CNT sheets is their use as a heating material [12–17]. The resistivity of CNT films can be controlled by the number of layers within the sheet or by the reagents used for their densification [17, 18]. CNTs can be incorporated into polymers to form composites for heating applications [16, 19]. However, CNT/polymer composites have a limited range of performance temperatures due to possible decomposition of the polymers [20]. Powdered CNTs dispersed in solvents have been used to coat cotton fabric and create CNT/textile heaters [21]. CNT-based heaters have also found applications as efficient and durable electrodes for Faradaic water splitting [22]. CNT sheet heaters have been fabricated as transparent film heaters, due to their high transmittance and good heating capabilities [12, 15–17]. CNT heaters have also demonstrated to be more efficient than commercial heating materials such as nichrome [18, 23]. Additionally, CNT-based heaters revealed rapid heating capabilities [23], which make them ideal candidates for applications in aerospace and heated clothing.

In this study, we fabricated CNT sheets from CNT arrays produced by the chemical vapor deposition (CVD) process. These sheets were densified by solvents and used for the manufacture of CNT heaters. The goal of this work is to study how the heater's design (number of layers in the CNT sheets, their post-processing) influences its performance, including the voltage required to generate heat and the rapid heating response. Finally, some possible applications of the CNT heater are provided in this study.

2. Experimental methods

CNT sheet fabrication started with the synthesis of vertically aligned, spinnable CNTs, typically about 400 μm in length. Thin films of Fe and Co were used as a catalyst (1.2 nm), which were sputtered on 4-inch Si wafers with 5-nm Al_2O_3 as a buffer sublayer. The obtained surface-engineered substrates were placed in a deposition reactor ET 3000 made by chemical vapor deposition (CVD) Equipment Corporation for the growth of the CNT arrays. Details of the growth process have been published elsewhere [24].

Upon completion of the CNT growth, detached, drawable CNT arrays were transferred onto an Si wafer or glass. CNT sheets with the desired number of layers were then assembled by continuously accumulating CNT ribbon onto a drum covered with a Teflon film as shown in **Figure 1**.

The resulting CNT sheets were densified, layer by layer, using acetone, as they were collected onto the drum. This solvent was used because a previous work showed that it can signifi-

http://dx.doi.org/10.5772/64054

cantly improve the electro-thermal behavior of CNT sheets [18]. Each revolution of the Teflon drum added one CNT layer of 50–70 nm thick ribbon onto the sheet. CNT sheets with various numbers of layers (1, 10, 100, 200 and 300) were produced by this technique.

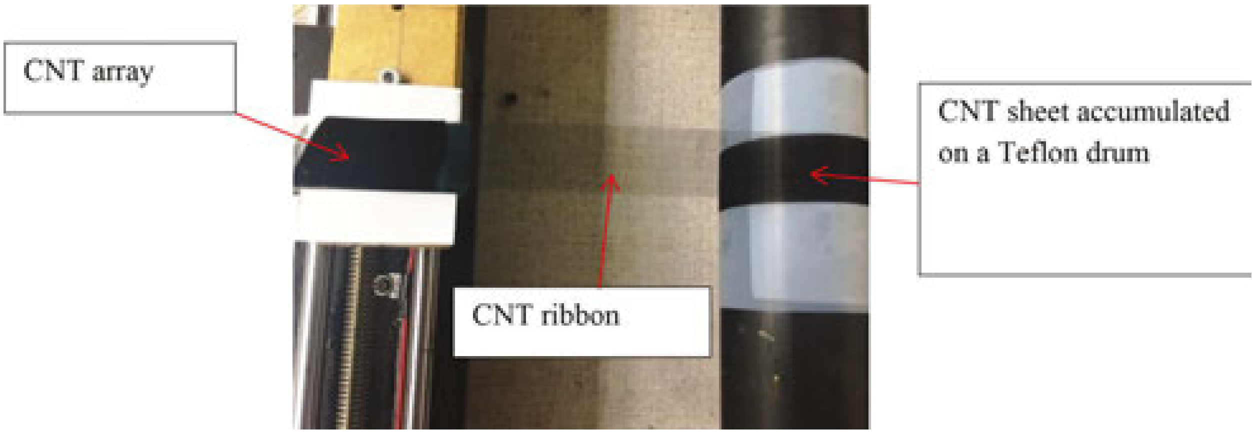

Figure 1. CNT ribbons being collected on a Teflon-covered drum from a CNT array.

CNT sheets were transferred onto a polyethylene terephthalate (PET) tape and then cut with a laser machine (Micro Machining Systems by Oxford Lasers, wavelength of 532 nm). PET tape was used as a supporting substrate, because this material is thermally stable up to 200°C and makes handling the CNT heaters easier. Samples were cut into 10 mm × 60 mm dimensions with a laser power of 5% and at a speed of 1 mm/s. The laser machine was also used to cut copper foils into 20 mm × 5 mm strips at a laser power of 40% and speed of 1 mm/s. The copper strips were attached at both ends of the CNT sheet with silver paste as shown in **Figure 2**, to form the CNT heater.

Figure 2. CNT sheet assembled between two polyethylene terephthalate (PET) tapes with Cu electrodes attached at both ends to form a CNT heater.

A DC power source (Hewlett Packard E 3612A) was used to supply power to the CNT heaters. The surface temperatures of the CNT heaters were measured using an infrared (IR) camera (FLIR T640). The average temperature was determined by measuring the surface temperature at three different locations across the sheet. The effective area of the CNT sheet actually heated up was 10 mm × 50 mm for all samples. The voltage was stepped until pre-determined heater temperatures were reached, and the corresponding current was measured. Measurements were taken at room temperature and pressure, after the heaters were allowed to reach an equilibrium temperature.

The sheet resistance of the CNT sheets was measured using a Jandel 4-probe instrument (Model RM3000). Prior to the measurement of the sheet resistance, samples were placed on a flat substrate, and then the sheet resistance was measured in the direction parallel and perpendicular to the alignment of the CNT sheet.

3. Results and discussion

3.1. Effect of the number of layers on sheet resistance

The sheet resistance of samples was measured in both parallel and perpendicular to the drawing directions, using four probe techniques, as shown in **Figure 3**. This method involves passing current through the two outer probes, while the resulting voltage drop is measured by the two inner probes. The measured sheet resistance is presented in **Table 1**.

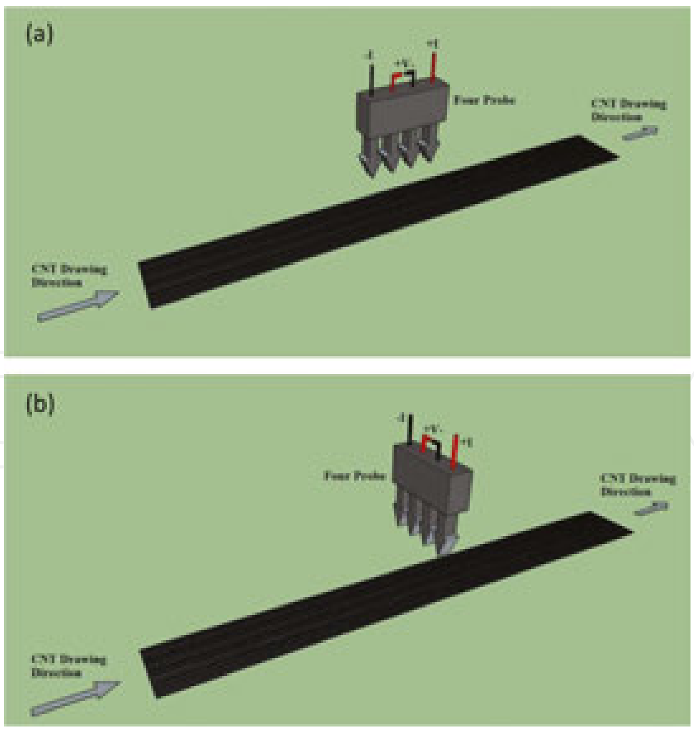

Figure 3. Scheme of the four-probe measurement applied to the CNT sheets in (a) parallel and (b) perpendicular to the drawing direction.

http://dx.doi.org/10.5772/64054

Number of layers	Parallel sheet resistance (Ω/sq.)	Perpendicular sheet resistance (Ω/sq.)
1	3567.80 ± 1413.03	3463.40 ± 727.35
10	171.26 ± 13.13	187.08 ± 21.72
100	17.21 ± 0.52	18.10 ± 0.39
200	9.89 ± 0.52	11.24 ± 0.69
300	6.03 ± 0.23	6.51 ± 0.18

Table 1. Resistance of CNT sheet in parallel and perpendicular to the drawing direction.

As the number of layers increased, the sheet resistance decreased accordingly. A growth in the number of layers leads to an increase in the density of CNTs, as shown by SEM images in **Figure 4**. The increase in density leads to a reduction in the electrical resistance, because the tube-to-tube contacts were increased, allowing for more electrons to be transferred through the sample.

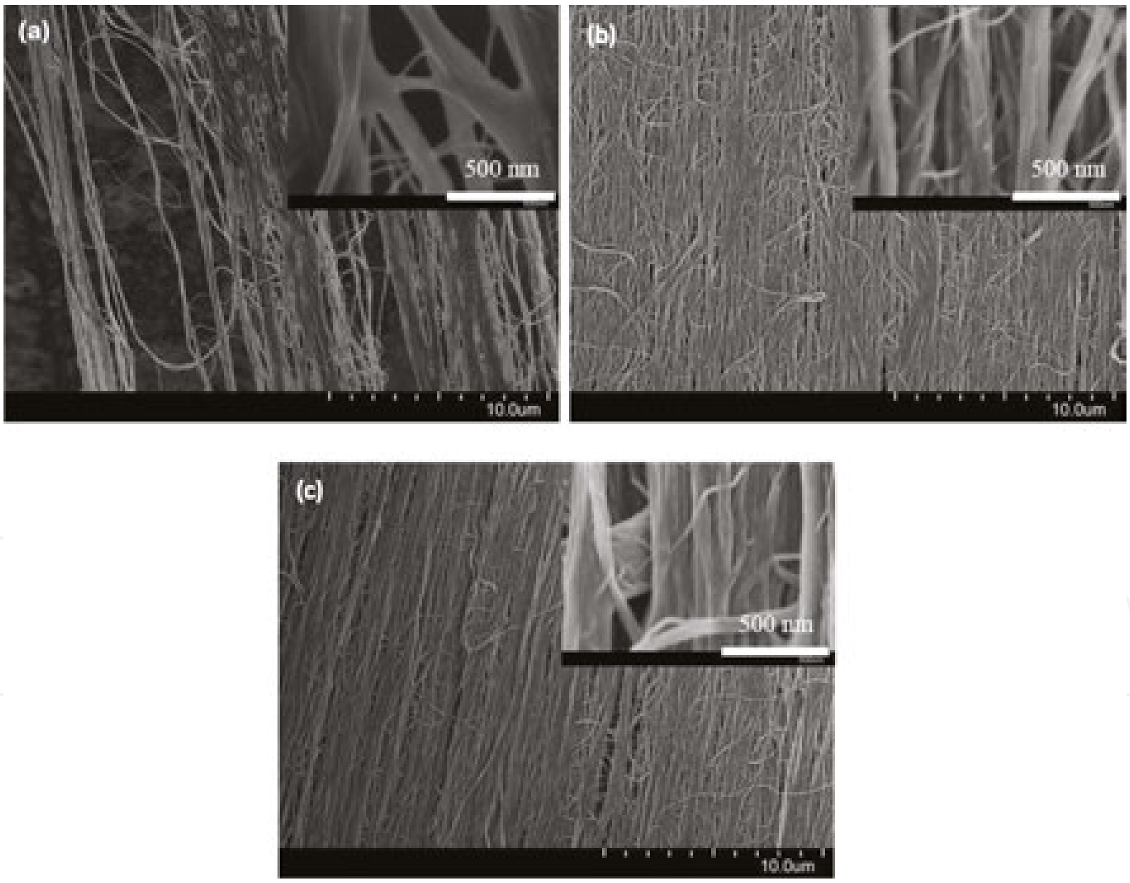

Figure 4. SEM images of (a) 1-, (b) 10- and (c) 100-layer-densified CNT sheets (high magnification in inset) showing an increase in density with increasing number of layers.

The parallel sheet resistance is lower than the perpendicular sheet resistance for 10, 100, 200 and 300 layers. This is because there is less resistance when electrons travel along the tube length, compared to the lateral tube-to-tube interactions, which take place in the perpendicular case. This is, however, not the case for a 1-layer sheet. As shown in **Figure 4a**, the probability of the 4 probes hitting the same bundle of sheets, to measure the resistance, is lower in the perpendicular direction compared to the parallel direction. The anisotropy of the sheets is, however, lower than what has been in reported in some cases. Inoue et al. reported an anisotropy of 7.3 between the sheet resistances in the parallel direction compared to that in the perpendicular direction [25].

3.2. Electrical properties of CNT heaters

The CNT sheets were connected to a DC power source, and the corresponding temperature was measured using an IR camera in ambient environment, as shown in **Figure 5**. The heat generated across the sheet is as a result of the Joule heating phenomenon. Joule heating is a phenomenon that occurs when electrical current is passed through a material with an electrical resistance. The resistance inherent to the material leads to a conversion of electrical energy to thermal energy. This is caused by the collision of the moving electrons with the atoms that are the main material's constituents. The quantity of heat (Q) that is yielded from the applied electrical energy is proportional to the square of the current (I) multiplied by the resistance (R) over a period of time (t) as per Eq. (1).

$$Q = I^2 R t \tag{1}$$

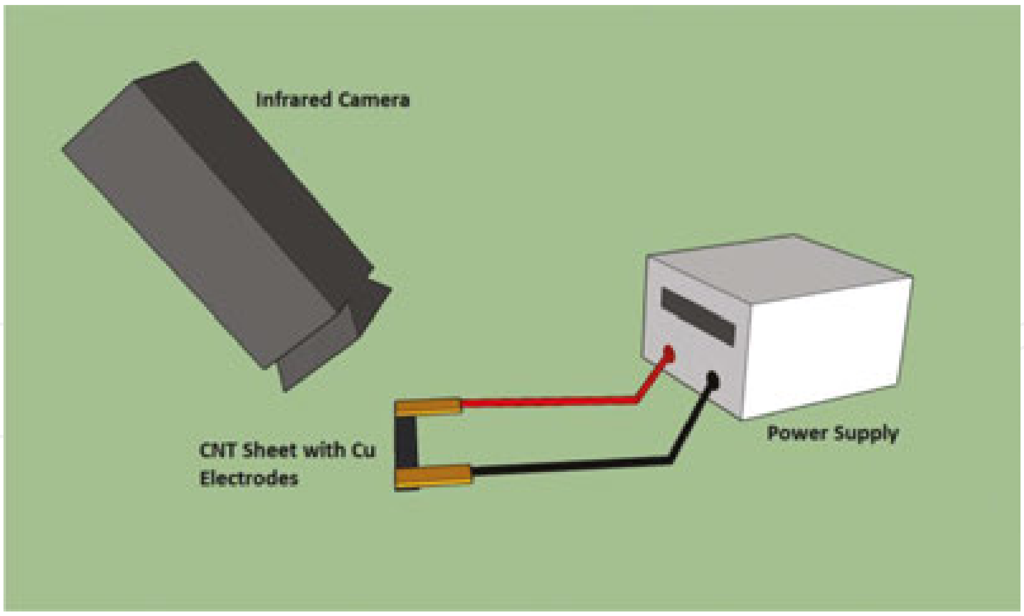

Figure 5. Schematic illustration of the temperature acquisition setup using an infrared (IR) camera.

However, we usually use another parameter, known as power (P), to describe how much electrical energy is converted into thermal energy. This is simply the quantity of heat (Q) divided by the time (t) as per Eq. (1), which leads to Eq. (2).

$$P = I^2 R = \frac{V^2}{R} \tag{2}$$

The power (P) generated by the CNT sheet when connected to a voltage source is also directly proportional to the voltage (V) across the sheet and the current (I) passing through the sheet (Eq. (2)). Different CNT heaters were connected to a DC power source, and the voltage was changed to correspond to temperatures 30, 50, 70, 90 and 110°C. The resultant current and voltage at each temperature were noted and used to calculate the corresponding power. The effect of the number of layers on the power needed to reach a particular temperature is illustrated in **Figure 6**. It can be seen that, as the number of layers increased, the power needed to generate a particular temperature also increased. This can be explained using Eq. (2), which shows that the resistance is inversely proportional to the power. An increase in the number of layers leads to a decrease in resistance, and this in turn leads to an increase in power needed to attain a particular temperature. Therefore, sheets with high resistance need a lower power to attain the same temperature as sheets with lower resistances.

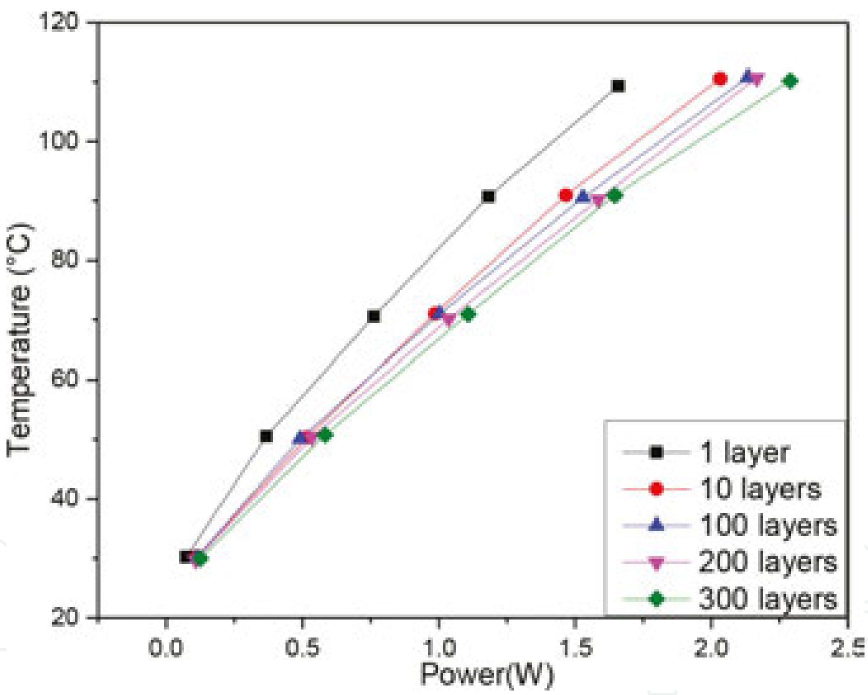

Figure 6. Power versus temperature for different number of layers within the CNT sheet.

Equation 2 also shows that the higher the resistance of the sheet, the greater the voltage needed to attain a specific temperature. This trend is clearly seen in **Figure 7**. The lower number layer sheets (1 and 10) needed very high voltages to attain the same temperature as the high number layer sheets (100, 200 and 300). For practical applications, the heater might be limited by the available low voltage supply. In such a case, CNT sheets with less number of layers would not be a feasible option, and higher number of layer sheets would be preferred.

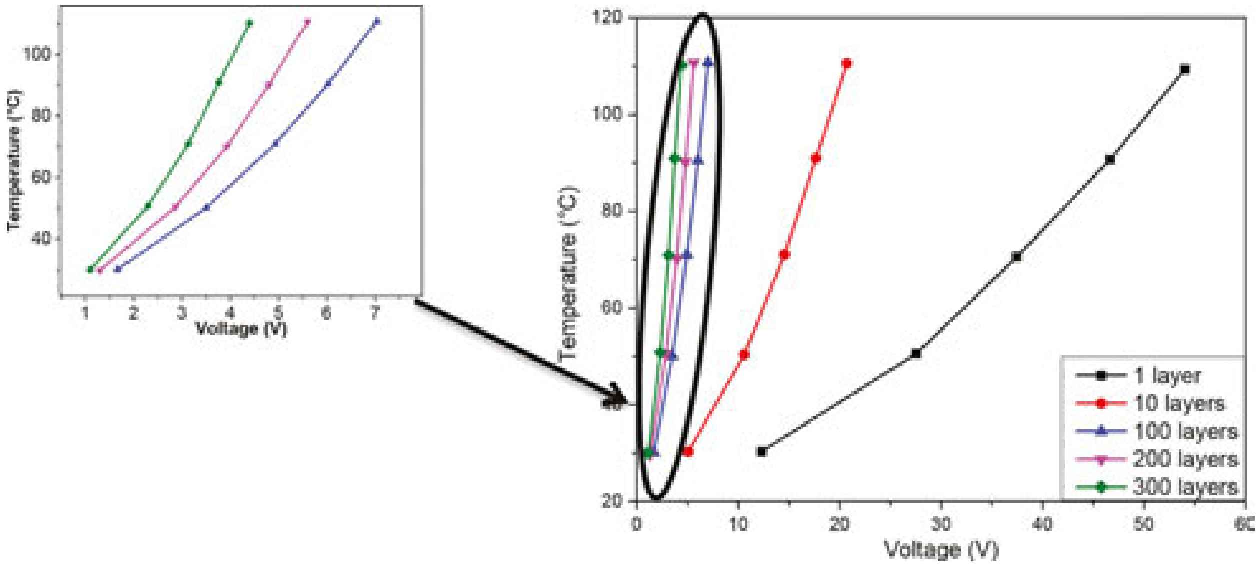

Figure 7. Voltage versus temperature for different number of layers within the CNT sheet.

The electrical resistivity of the CNT sheets was also investigated in this study. The resistivity (ρ) is related to the sheet resistance (R_s) and thickness (t) of the sheet by Eq. (3).

$$\rho = \frac{R_S}{t} \tag{3}$$

The resistivity of the CNT sheet can therefore be calculated if the thickness of the CNT sheet is known. Cross-sectional SEM images were taken on a selected number of samples to determine their thicknesses. The sheets were cut perpendicular to the drawing direction with a laser powered 0.5%, using a cutting speed of 0.1 mm/s.

The lower power and reduced speed of the laser were important to ensure a clean cut of the sheet and avoid pullouts of the CNTs disturbing the thickness uniformity. In order to increase the conductivity of the CNT sheets for SEM imaging, the samples were mounted on a vertical stub and coated with a thin layer of Au/Pd by a sputtering machine (Denton Vacuum Desk IV) using a sputtering time of 25 s. SEM images of the different sheet thicknesses are displayed in **Figure 8**. The SEM images show the CNT samples with uniform thickness across the sheet. The average thickness of 100, 200 and 300 layer sheets was 6.25, 13.32 and 20.31 μm, respectively. The calculated resistivity in the parallel direction using Eq. (2) for 100, 200 and 300 layer sheets was 1.08×10^{-2} Ω cm, 1.32×10^{-2} Ω cm, and 1.23×10^{-2} Ω cm, respectively. The resistivity of the sheets is comparable to the data reported in the literature where MWCNT films have been studied revealing a resistivity of 20×10^{-3} Ω cm [26]. Our resistivity is higher than those sheets composed of single-wall carbon nanotubes (SWCNTs), reported to be in the range of 10^{-4} to 10^{-5} Ω cm [4]. The high resistivity in our work is due to several factors, including the packing density of the nanotubes and the nature of the MWCNTs, which are less conductive than SWCNTs.

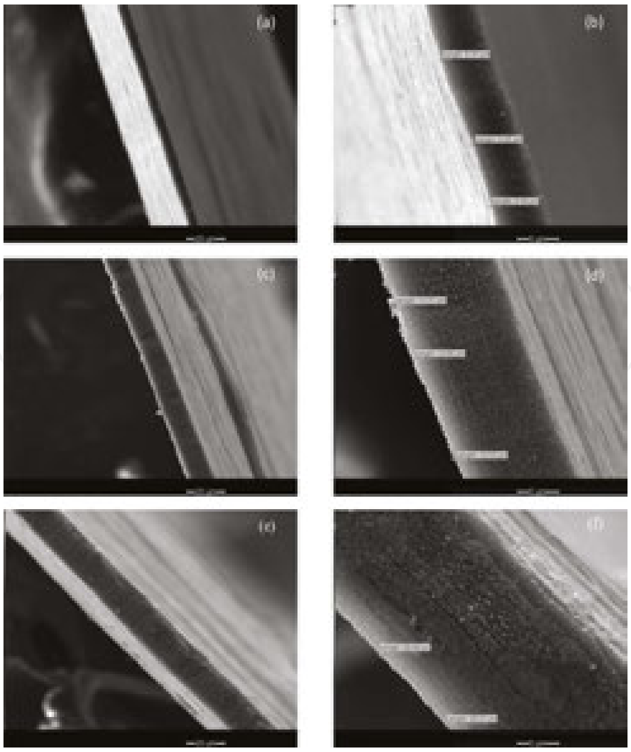

Figure 8. Cross-sectional SEM images showing the thickness of: (a) and (b) 100-layer CNT sheet; (c) and (d) 200-layer CNT sheet; and (e) and (f) 300-layer CNT sheet.

It has been shown in the literature that an improved packing density (by stretching and pressing) leads to improvement in electrical and mechanical properties [7, 27]. In the future, we intend to use these two approaches in order to increase the density of our CNT sheets and decrease their resistivity.

3.3. Temperature profile of CNT sheets

The heat generated by the CNT heater, when connected to a power source, is lost into the ambient environment during heating. The total heat is dissipated into the air and substrate through three mechanisms: conduction, convection and radiation [12].

The heating profiles with time of CNT sheets at selected low voltages (1.5, 3 and 4.5 V) are presented in **Figure 9**. The obtained data mimic possible low-voltage applications of the heaters. Sheets with 1 and 10 layers have not been included because they show negligible increase in temperature at the applied voltages.

The observed temperature evolution is divided into 3 stages: heating, saturation, and cooling. Cooling happens after the voltage source is turned off. During the saturation stage, the heat gained by the applied electric power is almost equal to the heat lost by radiation and convection. The average time for the heater to reach the temperature saturation is 20 s. However, the average cooling time depends on the final temperature of the heater and, therefore, varies, as shown in **Figure 9**. This fast heating time is a desirable characteristic of a heater that will be incorporated into clothing or textiles, to keep the body warm during cold seasons. This quality is also beneficial for deicing applications. We present some feasible applications of the CNT heaters created and studied in this work.

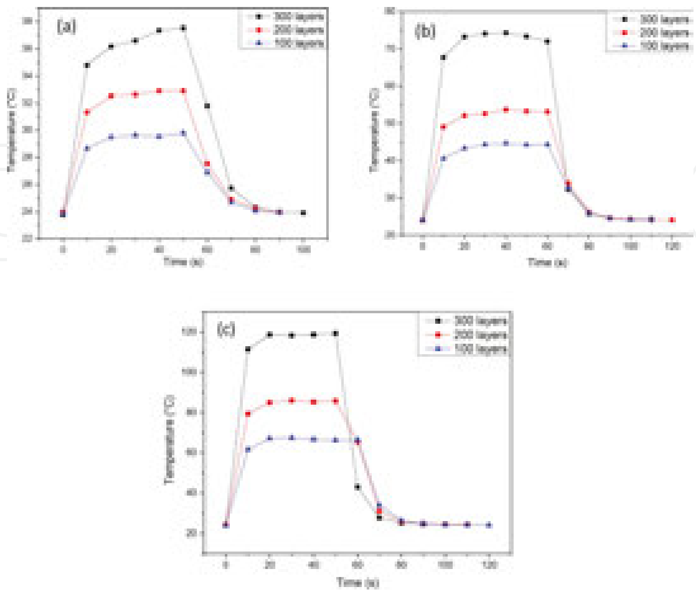

Figure 9. Heating profile as a function of time for 100-, 200- and 300-layer CNT sheets at (a) 1.5 V, (b) 3 V, and (c) 4.5 V.

4. Applications of CNT heaters

4.1. Heatable glove

CNT heaters are easy to design and manufacture, which makes them attractive for a variety of applications. Their lightweight, mechanical flexibility and low voltage make the CNT heaters appealing candidates for apparel, to protect operators performing in cold weather. We have fabricated CNT heaters and embedded them into gloves, based on the approach described in this work. The heaters were made using 200 and 150 layer sheets. Such gloves are lightweight since the CNT heaters do not add significant mass (total change of 1.21 g) and can also be operated with either a 9-V battery or a rechargeable Li-ion (2700 mAh, 3.7 V) battery, as shown in **Figure 10**. This type of application has advantages because of the ease of fabrication of the CNT heaters and the low voltage needed to power them.

4.2. Deicing applications

The use of CNT heaters for deicing applications was also studied. This approach was similar to that described by Janas et al. [23]. A 300-layer CNT heater was attached to the right wing of a model airplane. The test model was inserted into a freezer with a continuous voltage (3V) supply attached to the heater. Droplets of water were then sprinkled on both wings of the model airplane, shown in **Figure 11a**, and it was left in the freezer. The thermal image before ice formation is shown in **Figure 11b**, where the right wing temperature is above 0°C. After an hour of cooling, the wing without the CNT heater had visible ice formation on its surface, while the wing with the functioning heater was dry as shown in **Figure 11c**. The corresponding infrared image, after ice formation, is shown in **11d**, where the entire model airplane is frozen except for the right wing. This experiment shows that CNT heaters can be used in deicing applications to prevent the formation of ice on airplanes, which is a major issue in the aerospace industry. The heater can be incorporated into the surface of the fuselage, which is made of polymer composite for most of the military and some of the advanced commercial airplanes.

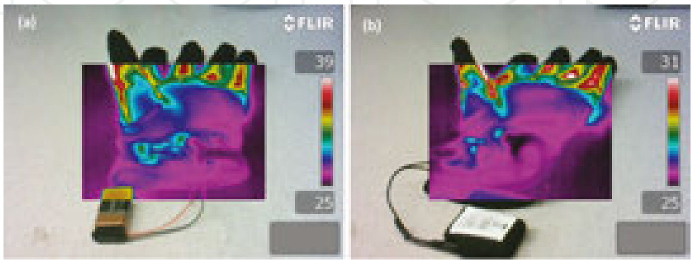

Figure 10. CNT-heated gloves connected to (a) 9-V battery and (b) rechargeable lithium ion battery. The color scale represents temperature in °C obtained by an IR camera.

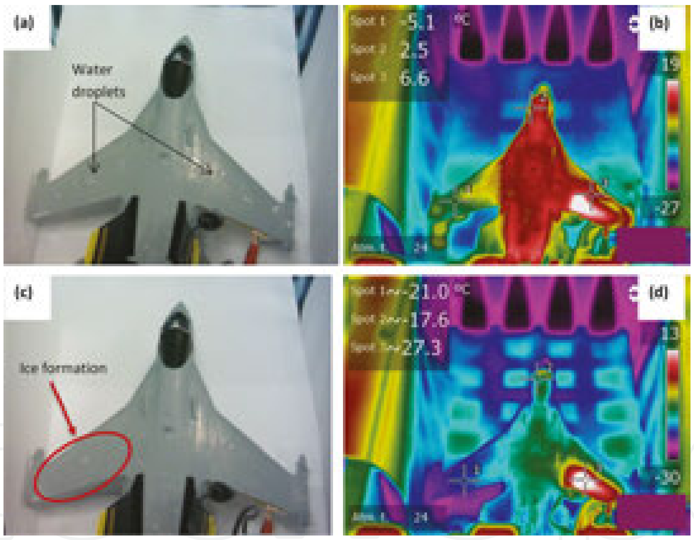

Figure 11. (a) Droplets of water on the wings of a model airplane with related (b) IR thermal image; (c) ice formation on the left wing of the model airplane after an hour of freezing and related (d) IR thermal image.

5. Conclusions

A simple and easy way for fabricating flexible and low-voltage CNT heaters was described. The resistance of the CNT sheets with different numbers of layers was studied. It was observed that as the number of layers increased, the sheet resistance decreased, showing that this property is dependent on the thickness of the sheet. The heating and cooling rates of these heaters were also studied. The obtained results suggested that the fast heating rate of the heaters makes them attractive for manufacturing body protection clothing used in cold weather. An example of the latter was demonstrated in this work by incorporating CNT heaters into a glove. Maximum glove temperatures of 39°C and 31°C were attained using a 9-V battery and Li-ion battery, respectively. Another application demonstrated that the CNT heater can find application in deicing solid surfaces exposed to freezing weather, such as airplanes. The CNT sheet heaters can be easily incorporated in polymer composites recently used as materials of choice for making advanced cars and fuselages.

Acknowledgements

This work was funded by the National Science Foundation (NSF) through the following grants: CMMI-0727250, SNM-1120382, ERC-0812348, and DURIP-ONR. The partial support by the National Institute for Occupational Safety and Health Pilot Research Project Training Program of the UC Education and Research Center Grant #T42/OH008432-10 is also acknowledged. The authors are grateful for the financial support from the UC Office of Research and the Mathewson Renewable Energy Research Fund. Seyram Gbordzoe is thankful for the graduate assistantship provided to him by the College of Engineering and Applied Science (CEAS) at UC and the Cincinnati Engineering Enhanced Mathematics and Science (CEEMS) program (NSF, DRL-1102990).

Author details

Seyram Gbordzoe[1], Rachit Malik[1], Noe Alvarez[2], Robert Wolf[3] and Vesselin Shanov[1,2*]

*Address all correspondence to: vesselin.shanov@uc.edu

1 Department of Mechanical and Materials Science Engineering, University of Cincinnati, Cincinnati, OH, USA

2 Department of Biomedical, Chemical and Environmental Engineering, University of Cincinnati, Cincinnati, OH, USA

3 Department of Electrical Engineering, University of Cincinnati, Cincinnati, OH, USA

References

[1] Iijima, S., *Helical microtubules of graphitic carbon*. Nature, 1991. 354(6348): pp. 56–58.

[2] Jung , D., M. Han, L.J. Overzet, and G.S. Lee, *Effect of hydrogen pretreatment on the spin-capability of a multiwalled carbon nanotube forest*. Journal of Vacuum Science & Technology B, 2013. 31(6): p. 06FI02.

[3] Treacy, M.M.J., T.W. Ebbesen, and J.M. Gibson, *Exceptionally high Young's modulus observed for individual carbon nanotubes*. Nature, 1996. 381(6584): pp. 678–680.

[4] Ebbesen, T.W., H.J. Lezec, H. Hiura, J.W. Bennett, H.F. Ghaemi, and T. Thio, *Electrical conductivity of individual carbon nanotubes*. Nature, 1996. 382(6586): pp. 54–56.

[5] Jung, D., M. Han, and G.S. Lee, *Gas sensor using a multi-walled carbon nanotube sheet to detect hydrogen molecules*. Sensors and Actuators A: Physical, 2014. 211: pp. 51–54.

[6] Pöhls, J.-H., M.B. Johnson, M.A. White, R. Malik, B. Ruff, C. Jayasinghe, M.J. Schulz, and V. Shanov, *Physical properties of carbon nanotube sheets drawn from nanotube arrays*. Carbon, 2012. 50(11): pp. 4175–4183.

[7] Liu, Q., M. Li, Y. Gu, Y. Zhang, S. Wang, Q. Li, and Z. Zhang, *Highly aligned dense carbon nanotube sheets induced by multiple stretching and pressing*. Nanoscale, 2014. 6(8): pp. 4338–4344.

[8] Zhang, M., S. Fang, A.A. Zakhidov, S.B. Lee, A.E. Aliev, C.D. Williams, K.R. Atkinson, and R.H. Baughman, *Strong, transparent, multifunctional, carbon nanotube sheets*. Science, 2005. 309(5738): pp. 1215–1219.

[9] Chun, K.-Y., et al., *Hybrid carbon nanotube yarn artificial muscle inspired by spider dragline silk*. Nat Commun, 2014. 5(3322).

[10] Zhang, M., K.R. Atkinson, and R.H. Baughman, *Multifunctional carbon nanotube yarns by downsizing an ancient technology*. Science, 2004. 306(5700): pp. 1358–1361.

[11] Jayasinghe, C., T. Amstutz, M.J. Schulz, and V. Shanov, *Improved processing of carbon nanotube yarn*. Journal of Nanomaterials, 2013. 2013: p. 7.

[12] Jung, D., M. Han, and G.S. Lee, *Flexible transparent conductive heater using multiwalled carbon nanotube sheet*. Journal of Vacuum Science & Technology B, 2014. 32(4): p. 04E105.

[13] Wu, Z., Q. Xu, J. Wang, and J. Ma, *Preparation of large area double-walled carbon nanotube macro-films with self-cleaning properties*. Journal of Materials Science & Technology, 2010. 26(1): pp. 20–26.

[14] Jang, H.-S., S.K. Jeon, and S.H. Nahm, *The manufacture of a transparent film heater by spinning multi-walled carbon nanotubes*. Carbon, 2011. 49(1): pp. 111–116.

[15] Kim, D., H.-C. Lee, J.Y. Woo, and C.-S. Han, *Thermal behavior of transparent film heaters made of single-walled carbon nanotubes*. The Journal of Physical Chemistry C, 2010. 114(13): pp. 5817–5821.

[16] Kim, D., L. Zhu, D.-J. Jeong, K. Chun, Y.-Y. Bang, S.-R. Kim, J.-H. Kim, and S.-K. Oh, *Transparent flexible heater based on hybrid of carbon nanotubes and silver nanowires*. Carbon, 2013. 63: pp. 530–536.

[17] Jung, D., D. Kim, K.H. Lee, L.J. Overzet, and G.S. Lee, *Transparent film heaters using multi-walled carbon nanotube sheets*. Sensors and Actuators A: Physical, 2013. 199: pp. 176–180.

[18] Dawid Janas and Krzysztof K. Koziol, "Improved Performance of Ultra-Fast Carbon Nanotube Film Heaters," Jounal of Automation and Control Engineering, Vol. 2, No. 2, pp. 150–153 June, 2014. doi: 10.12720/joace.2.2.150–153.

[19] Kunmo, C., K. Dongouk, S. Yoonchul, L. Sangeui, M. Changyoul, and P. Sunghoon, *Electrical and thermal properties of carbon-nanotube composite for flexible electric heating-unit applications*. Electron Device Letters, IEEE, 2013. 34(5): pp. 668–670.

[20] Lee, E. and Y.G. Jeong, *Preparation and characterization of sulfonated poly(1,3,4-oxadiazole)/multi-walled carbon nanotube composite films with high performance in electric heating and thermal stability*. Composites Part B: Engineering, 2015. 77: pp. 162–168.

[21] Ilanchezhiyan, P., A.S. Zakirov, G.M. Kumar, S.U. Yuldashev, H.D. Cho, T.W. Kang, and A.T. Mamadalimov, *Highly efficient CNT functionalized cotton fabrics for flexible/wearable heating applications*. RSC Advances, 2015. 5(14): pp. 10697–10702.

[22] Janas, D., S. Kreft, S. Boncel, and K.K. Koziol, *Durability and surface chemistry of horizontally aligned CNT films as electrodes upon electrolysis of acidic aqueous solution*. Journal of Materials Science, 2014. 49(20): pp. 7231–7243.

[23] Janas, D. and K.K. Koziol, *Rapid electrothermal response of high-temperature carbon nanotube film heaters*. Carbon, 2013. 59: pp. 457–463.

[24] Alvarez, N.T., P. Miller, M. Haase, N. Kienzle, L. Zhang, M.J. Schulz, and V. Shanov, *Carbon nanotube assembly at near-industrial natural-fiber spinning rates*. Carbon, 2015. 86: pp. 350–357.

[25] Inoue, Y., Y. Suzuki, Y. Minami, J. Muramatsu, Y. Shimamura, K. Suzuki, A. Ghemes, M. Okada, S. Sakakibara, and H. Mimura, *Anisotropic carbon nanotube papers fabricated from multiwalled carbon nanotube webs*. Carbon, 2011. 49(7): pp. 2437–2443.

[26] Bacsa, W., A. Chatelain, T. Gerfin, R. Humphrey-Baker, L. Forro, and D. Ugarte, *Aligned carbon nanotube films: production and optical and electronic properties*. Science, 1995. 268(5212): pp. 845–847.

[27] Cheng, Q., J. Bao, J. Park, Z. Liang, C. Zhang, and B. Wang, *High mechanical performance composite conductor: multi-walled carbon nanotube sheet/bismaleimide nanocomposites*. Advanced Functional Materials, 2009. 19(20): pp. 3219–3225.